

# Flow force and torque on submerged bodies in lattice-Boltzmann via momentum exchange

Juan P. Giovacchini<sup>1,3\*</sup> and Omar E. Ortiz<sup>2,3†</sup>

<sup>1</sup>*Departamento de Mecánica Aeronáutica, Instituto Universitario Aeronáutico, Córdoba, Argentina.*

<sup>2</sup>*Facultad de Matemática, Astronomía y Física, Universidad Nacional de Córdoba, Argentina.*

<sup>3</sup>*Instituto de Física Enrique Gaviola (CONICET), Córdoba, Argentina.*

We present a new derivation of the momentum exchange algorithm first introduced by Ladd [12], to compute the flow force and torque on a submerged body. The starting point of our derivation is to consider the time derivative of the total momentum of a *virtual* fluid system that replaces the submerged body in the real problem. The new derivation gives, in turn, some correction terms to the original algorithm. We also present numerical tests that support the correctness of the formulas derived.

PACS numbers: 47.11.-j, 47.10.-g, 51.10.+y

## I. INTRODUCTION

During the last twenty-five years the Lattice-Boltzmann methods (*LBM*) have been greatly developed in many aspects. Today they can be used, to treat multiple problems involving both compressible and incompressible flows on simple and complex geometrical settings.

It is of crucial importance, in many applications that involve moving bodies surrounded by a fluid flow, to have a good method or algorithm to compute the flow force and torque acting on the bodies. By good we mean a method that is simple to apply, that is accurate and fast, so as not to spoil the efficiency of the flow computing method.

The classical way to compute forces, and so torque, on submerged bodies is via the computation and integration of the stress tensor on the surface of the body. In LBM the stress tensor is not a natural variable, its computation and extrapolation from the lattice to the surface is computationally expensive, which ruins the efficiency of the LBM. However, this method is widely used in LBM [11, 15, 24].

In 1994 Ladd introduced a new method, the *momentum exchange (ME)*, to compute the flow force on a submerged body [12, 13]. Ladd's idea was rather heuristic and very successful, where the force is obtained by accounting the exchange of momentum between the surface of the body and the fluid, the latter being represented by "fluid particles" whose momentum is easily written in terms of the LBM variables that describe the fluid at the mesoscopic scale. The ME algorithm is specifically designed and adapted to LBM; it is therefore more efficient than stress integration from the computational point of view.

The ME algorithm has been tested and applied successfully to a variety of problems [13, 14, 18]. Some accuracy

problems have been detected though, when applied to moving bodies [15, 22]. The main goal of this paper is to provide a formal derivation of the momentum exchange algorithm. This new derivation provides in turn, some corrections to the original Ladd's formula and also to some newer, improved versions of momentum exchange algorithm that have been proposed [22]. Instead of start thinking in the variables at mesoscopic level, we start by considering the time derivative the total momentum of a *virtual* fluid system that replaces the submerged body under consideration.

The rest of the paper is organized as follows. In section II we briefly discuss the lattice-Boltzmann method with the main purpose of introducing notation; the method used to treat boundary conditions is also explained in this section. In Section III, the core of the paper, we present our derivation of the momentum exchange method to determine both, the flow force and torque on static or moving bodies. In section IV we present three numerical tests where we implement the methods derived in section III. We compare our results with those obtained with the original Ladd's algorithm, and also with results obtained by other authors using various methods of computational fluid dynamics. In section V we make some comments.

## II. THE LATTICE-BOLTZMANN METHOD

In this section we present the basic equations of the lattice Boltzmann methods with the main purpose of introducing the notation used along the paper. For a thorough description of the Boltzmann equation we refer to [7, 19]. For a more complete presentation of LBM we refer to [9, 20, 23].

The Boltzmann equation (*BE*) governs the time evolution of the single-particle distribution function  $f(\mathbf{x}, \boldsymbol{\xi}, t)$ , where  $\mathbf{x}$  and  $\boldsymbol{\xi}$  are the position and velocity in phase space. The lattice Boltzmann equation (*LBE*) is a discretized version of the Boltzmann equation, where  $\mathbf{x}$  takes values on a uniform grid (the lattice), and  $\boldsymbol{\xi}$  is not only discretized, but also restricted small number of values [10]. By far the models used most frequently are

\*Electronic address: giovacchini@famaf.unc.edu.ar

†Electronic address: ortiz@famaf.unc.edu.ar

the ones with collision integral simplified according to the Bhatnagar, Gross, and Krook (*BGK*) approximation [1] and with single relaxation time (*SRT*)  $\tau$ . In an isothermal situation and in the absence of external forces, like gravity, the LBE of this models read

$$f_i(\mathbf{x}_A + \mathbf{c}_i \delta t, t + \delta t) = f_i(\mathbf{x}_A, t) - \frac{1}{\tau} \left( f_i(\mathbf{x}_A, t) - f_i^{eq}(\mathbf{x}_A, \rho, \mathbf{u}, t) \right),$$

$$i = 0, 1, \dots, Q-1. \quad (1)$$

Here  $f_i = \omega_i f(\mathbf{x}_A, \mathbf{c}_i, t)$  is the  $i$ -th component of the discretized distribution function at the lattice site  $x_A$ , time  $t$ , and corresponding to the discrete velocity  $\mathbf{c}_i$ .  $\omega_i$  is the  $i$ -th quadrature weight (explained below), and  $Q$  the number of discrete velocities in the model. In compressible-flow models the lattice constant  $\delta x$ , that separate two nearest neighbor nodes, and the time step  $\delta t$  are related with the speed of sound  $c/\sqrt{3}$  by  $\delta x = c \delta t$  [26]. The coordinates of a lattice node are  $\mathbf{x}_A$ , where the integer multi index  $A = (j, k, l)$  (or,  $A = (j, k)$  in the two-dimensional case) denotes a particular site in the lattice. The equilibrium distribution function  $f^{eq}$  is a truncated Taylor expansion of the Maxwell-Boltzmann distribution. It is this approximation what makes LBM accurate only at low Mach numbers [10].

The macroscopic quantities such as the fluid mass density  $\rho(\mathbf{x}, t)$ , and velocity  $\mathbf{u}(\mathbf{x}, t)$ , are obtained, in Boltzmann theory, as marginal distributions of  $f$  and  $\xi f$  when integrating over  $\xi$ . In LBM this integrals are approximated by proper quadratures. Specific values of  $c_i$ 's and  $\omega_i$ 's,  $i = 0, 1, \dots, Q-1$ , are made so that these quadratures give exact results for the  $\xi$ -moments of order 0, 1 and 2 [10, 23]. We have

$$\rho(\mathbf{x}_A, t) = \sum_{i=0}^{Q-1} f_i(\mathbf{x}_A, t), \quad (2)$$

and

$$\rho \mathbf{u}(\mathbf{x}_A, t) = \sum_{i=0}^{Q-1} \mathbf{c}_i f_i(\mathbf{x}_A, t). \quad (3)$$

In the simulations we present in this paper, we are interested in incompressible flow problems, where we modify Eq. 3 according to the quasi-incompressible approximation presented in [8]. In this approximation  $\rho$  is replaced by  $\rho_0$ , a constant fluid mass density.

A single time step of the discrete evolution equation (1) is frequently written as a two-stage process

$$\hat{f}_i(\mathbf{x}_A, t) = f_i(\mathbf{x}_A, t) - \frac{1}{\tau} \left( f_i(\mathbf{x}_A, t) - f_i^{eq}(\mathbf{x}_A, \rho, \mathbf{u}, t) \right), \quad (4)$$

and

$$f_i(\mathbf{x}_A + \mathbf{c}_i \delta t, t + \delta t) = \hat{f}_i(\mathbf{x}_A, t). \quad (5)$$

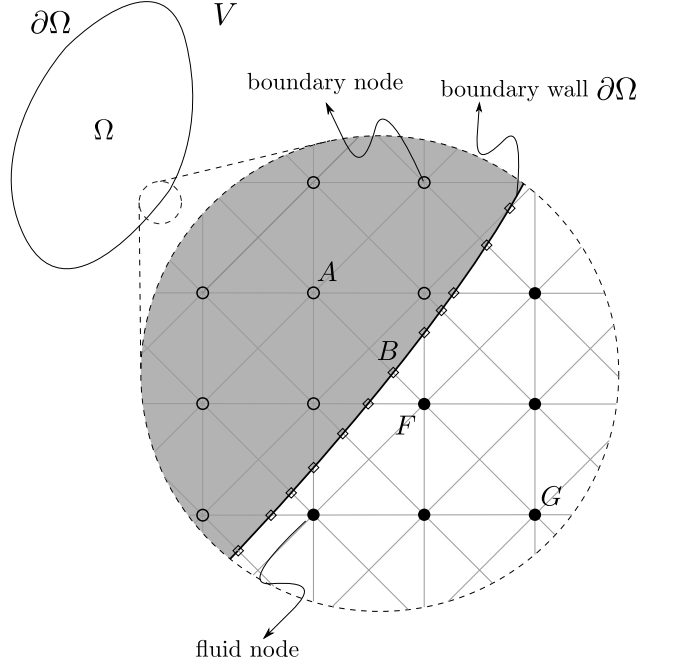


FIG. 1: Detail of boundary region, surrounding fluid and lattice.

The computation of  $\hat{f}_i$  on the whole lattice, Eq. (4), is called the *collision step*, while the computation of  $f_i$  at  $t + \delta t$ , Eq. (5), on the whole lattice is called *streaming step*.

Two results that we frequently use are

$$\sum_i \hat{f}_i(\mathbf{x}_A, t) = \sum_i f_i(\mathbf{x}_A, t), \quad (6)$$

$$\sum_i \mathbf{c}_i \hat{f}_i(\mathbf{x}_A, t) = \sum_i \mathbf{c}_i f_i(\mathbf{x}_A, t), \quad (7)$$

that follow from the properties of the integral collision operator [7, 19] and Eq. (1).

### A. Treatment of boundary conditions

Many methods have been proposed in the literature to implement boundary conditions on moving boundaries with complex geometries in LBM. The method introduced in [5], later improved in [16, 17], has been extensively tested and is the one we use in the simulations presented in this paper. We explain this method briefly in what follows[27].

We consider a body  $\Omega$  with closed boundary  $\partial\Omega$  immersed in a fluid flow, and concentrate in a small portion of the boundary and its surrounding fluid as shown in Figure 1. The lattice nodes and links are also shown in the figure. Empty circles represent nodes lying inside the body, while filled circles represent nodes lying in the fluid region at the time shown. At time  $t$  a piece of boundary

lie, in general, between lattice nodes. Consider a node  $F$  on the fluid with a neighbour node  $A$  inside the body. To determine the values of  $f_i(\mathbf{x}_F = \mathbf{x}_A + \mathbf{c}_i \delta t, t + \delta t)$ , the streaming step needs “non-existent” information coming from node  $A$ . It is the application of the boundary conditions what provides this information with the desired accuracy. The method presented in [5] proposes to determine  $\hat{f}_i(\mathbf{x}_A, t)$  so that the linearly interpolated velocity at the boundary point  $B$  is the correct boundary velocity at that point. This is

$$\hat{f}_i(\mathbf{x}_A, t) = (1 - \chi) \hat{f}_{\bar{i}}(\mathbf{x}_A + \mathbf{c}_i \delta t) + \chi g_{\bar{i}}(\mathbf{x}_A, t) + 2\omega_{\bar{i}} \rho \frac{3}{c^2} \mathbf{c}_{\bar{i}} \cdot \mathbf{u}_B \quad (8)$$

where  $\bar{i}$  denotes the index for the opposite direction to  $\mathbf{c}_i$  (i.e.,  $\mathbf{c}_{\bar{i}} = -\mathbf{c}_i$ ), and

$$g_{\bar{i}}(\mathbf{x}_A, t) = \omega_{\bar{i}} \rho (\mathbf{x}_A + \mathbf{c}_i \delta t) \left( 1 + \frac{3}{c^2} \mathbf{c}_{\bar{i}} \cdot \mathbf{u}_{bf} + \frac{9}{2c^4} (\mathbf{c}_{\bar{i}} \cdot \mathbf{u}_F)^2 - \frac{3}{2c^2} \mathbf{u}_F \cdot \mathbf{u}_F \right) \quad (9)$$

is a fictitious equilibrium distribution function at the fluid node  $A$ .  $\omega_i$ ,  $i = 0, 1, \dots, Q-1$ , are the weight factors of the LBM method.  $\mathbf{u}_B = \mathbf{u}(\mathbf{x}_B, t)$  and  $\mathbf{u}_F = \mathbf{u}(\mathbf{x}_F, t)$  are the boundary and fluid velocities respectively, with  $\mathbf{x}_B$  the intersection point between the boundary and the link joining  $A$  with  $F$ . Different choices of  $\mathbf{u}_{bf}$ , a velocity between  $\mathbf{x}_B$  and  $\mathbf{x}_F$ , give alternative values of the parameter  $\chi$ , the weighting factor that controls the interpolation (or extrapolation). To improve numerical stability [16, 17] propose

$$\mathbf{u}_{bf} = \mathbf{u}_G = \mathbf{u}(\mathbf{x}_F + \mathbf{c}_i \delta t, t), \quad \chi = \frac{2\Delta - 1}{\tau - 2}, \quad \text{if } \Delta < \frac{1}{2},$$

and

$$\mathbf{u}_{bf} = \mathbf{u}_F + \frac{3}{2\Delta} (\mathbf{u}_B - \mathbf{u}_F), \quad \chi = \frac{2\Delta - 1}{\tau + \frac{1}{2}}, \quad \text{if } \Delta \geq \frac{1}{2},$$

where  $0 \leq \Delta \leq 1$  is the fractional distance

$$\Delta = \frac{\|\mathbf{x}_F - \mathbf{x}_B\|}{\|\mathbf{x}_F - \mathbf{x}_A\|}. \quad (10)$$

Lattice nodes on either side of the boundary surface are treated as fluid nodes. This is, we think the body region  $\Omega$  as if it was filled with fluid; an idea that will be essential in our derivation of the momentum exchange formulas in section III A. The idea of having fluid on both sides of the boundary simplifies the computational process, especially to overcome the problem of creating and destroying fluid when a node changes domain. An alternative way to treat the fluid close to boundaries is to evolve only outside the body and using, for example, the proposal of [2, 14] to update the nodes that change domain.

## B. Forces evaluation in lattice Boltzmann method

It is of great interest to have a robust, accurate method to compute flow forces in fluid mechanics. Several algorithms have been proposed to carry out this in the context of LBM. Many of these procedures fall in one of the categories: stress integration (*SI*) or momentum exchange (*ME*). Stress integration is based on the classical hydrodynamic approach (see e.g., [11]). Momentum exchange, introduced by Ladd [12], was specifically designed for LBM and has been implemented and tested in many fluid-mechanical problems. We will refer to Ladd’s original method as *original momentum exchange (OME)*.

OME was introduced as a heuristic algorithm by thinking the flow as composed by “fluid particles” and using particle dynamics to describe their interaction with the boundaries. Its implementation strictly depends on how the boundary conditions are treated. OME works well in many fluid-mechanical problems involving static and moving geometries. To the knowledge of the authors there are many applications and tests of OME, but no clear derivation of it in the literature. The work of Caiazzo and Junk present an analysis of ME that uses an asymptotic expansion [3].

The computational performance of OME is higher than that of SI. In SI one needs to compute the stress tensor in all lattice nodes which are first neighbors of the body surface. One then needs to extrapolate the stress tensor to the surface, and finally obtain the total flow force on the body as an integral over the whole body surface. In OME the procedure is simpler. The total force on the body is the sum of all contributions due to momentum change, in the directions pointing towards the body surface, over all lattice nodes in the fluid which are neighbors to the body surface.

Some accuracy problems have been found when applying OME to determine the force acting on moving bodies [15]. To overcome these inaccuracies, Wen et. al. [22] have proposed an ad-hoc correction to OME that apparently improve the accuracy of the computed force acting on moving bodies. In this work we give a demonstration of ME, from a fluid mechanics perspective, in which correction terms for OME are found. We find that the corrections proposed in [22] are partially adequate.

## III. MOMENTUM EXCHANGE METHOD

We want to simulate a fluid flow and submerged body motion within a region of space that we denote by  $V$ . We consider  $V$  to be a fixed region of space as seen on an inertial reference frame. We have covered  $V$  with a uniform constant lattice to solve the fluid motion by applying the lattice-Boltzmann method as described in section II.

The submerged body occupies a sub-region  $\Omega(t) \subset V$  that we consider, along the whole simulation, strictly contained in  $V$ . As the time dependence indicates,  $\Omega(t)$

doesn't need to be fixed.  $\Omega(t)$  can move and could even change shape. In this paper we work with rigid bodies, though this rigidity assumption is not essential and can be relaxed. The treatment presented below for moving bodies includes the case of non rigid bodies.

Without loss of generality, the movement of the body is assumed to be prescribed along this derivation, i.e.,  $\Omega$  is given as function of  $t$ . During an actual computation the body movement is determined by integrating the equations of motion of the body simultaneously with the flow equations. The equations of motion of the body take into account the fluid force on the body, the bulk forces like weight, etc.

The boundary of the body  $\partial\Omega$  is a moving, physical boundary for the flow. The flow everywhere is determined in such a way that the right boundary conditions are satisfied on  $\partial\Omega$  while  $\partial\Omega$  moves as prescribed by  $\Omega(t)$ .

In the rest of this section we present a derivation of the momentum exchange method for both, static and moving bodies.

### A. Fluid force on a submerged body

To derive the force on the submerged body we turn to the following idea. We assume that the region  $\Omega(t)$  is, instead of a submerged body, a portion of the same fluid whose flow is under study. We think of  $\Omega(t)$  as a fluid or material system, as generally understood in fluid mechanics (see [6], chapter 1), that moves inside a flow of a surrounding fluid of the same nature. The fluid flow inside  $\Omega$  is such that the right boundary conditions are satisfied at  $\partial\Omega$ , in particular, no mass crosses the system boundary  $\partial\Omega$ . The interior and exterior flows together determine that the movement of  $\partial\Omega$  is exactly as prescribed by  $\Omega(t)$ . Then, the time rate of change of the total momentum of the fluid inside  $\Omega$  equals the exterior flow force acting on  $\partial\Omega$ . This flow force is the same that would be obtained by projecting the stress tensor of the outer fluid in the normal direction to the surface and integrating over  $\partial\Omega$ . We refer the fluid system inside  $\Omega(t)$  as a *virtual fluid*, as this idea closely resembles that of *virtual charges* used in electrostatic theory to construct potentials with prescribed equipotential surfaces.

The accuracy of the computed force will clearly depend on how accurate the imposition of boundary conditions at  $\partial\Omega$  is. Our derivation of ME is independent of how boundary conditions are treated, though. Only when ME is applied one needs to make a particular choice of treatment for the boundary conditions. In this work, to perform the numerical tests, we impose the boundary conditions as described in section II A.

The total momentum of the virtual fluid, i.e. the fluid system inside  $\Omega$ , is

$$\mathbf{P}(t) = \int_{\Omega(t)} \mathbf{u}(\mathbf{x}, t) \rho(\mathbf{x}, t) d\mathbf{x}. \quad (11)$$

Thus, the time rate of change of the momentum of  $\Omega$  can

be expressed as

$$\frac{d\mathbf{P}}{dt} = \frac{1}{\delta t} \left( \int_{\Omega(t+\delta t)} (\mathbf{u}\rho)(\mathbf{x}, t+\delta t) d\mathbf{x} - \int_{\Omega(t)} (\mathbf{u}\rho)(\mathbf{x}, t) d\mathbf{x} \right) + \mathcal{O}(\delta t). \quad (12)$$

Space integrals are discretized as sums over the lattice [28]. Let  $\delta V$  be the volume associated to a single lattice cell. The lattice size is constant, related to the time step by  $\delta x = c\delta t$ , and  $\delta V = \delta x^D$ , being  $D$  the number of space dimensions. This uniformity assumption is not a restriction to treat problems with different scales. If necessary, one can use mesh refinement for example. In this case one needs to take it into account the constant relation between the lattice size and the time step.

Calling  $\mathcal{A}_t$  the set of all nodes  $A$  inside  $\Omega(t)$ , using (3) and neglecting the terms of order  $\mathcal{O}(\delta t)$ , we have

$$\begin{aligned} \mathbf{F} &\simeq \frac{\delta V}{\delta t} \left( \sum_{A \in \mathcal{A}_{t+\delta t}} \sum_i \mathbf{c}_i f_i(\mathbf{x}_A, t+\delta t) - \sum_{A \in \mathcal{A}_t} \sum_i \mathbf{c}_i f_i(\mathbf{x}_A, t) \right) \\ &\simeq \frac{\delta V}{\delta t} \sum_i \mathbf{c}_i \left( \sum_{A \in \mathcal{A}_{t+\delta t}} f_i(\mathbf{x}_A, t+\delta t) - \sum_{A \in \mathcal{A}_t} f_i(\mathbf{x}_A, t) \right), \end{aligned}$$

which, by (5), can be written as

$$\mathbf{F} \simeq \frac{\delta V}{\delta t} \sum_i \mathbf{c}_i \left( \sum_{A \in \mathcal{A}_{t+\delta t}} \hat{f}_i(\mathbf{x}_A - \mathbf{c}_i \delta t, t) - \sum_{A \in \mathcal{A}_t} f_i(\mathbf{x}_A, t) \right). \quad (13)$$

With assumptions done so far, Eq. (13) is a general expression to evaluate the flow force acting over a static or moving body. We discuss in what follows the cases of static and moving, submerged body.

#### 1. Static body

If the body does not move,  $\Omega$  and  $\mathcal{A}$  are independent of  $t$ . Eq. (13) becomes

$$\mathbf{F} \simeq \frac{\delta V}{\delta t} \sum_i \mathbf{c}_i \sum_{A \in \mathcal{A}} \left( \hat{f}_i(\mathbf{x}_A - \mathbf{c}_i \delta t, t) - f_i(\mathbf{x}_A, t) \right). \quad (14)$$

Notice that  $\hat{f}_i$  is evaluated at nodes which are all displaced exactly by an amount  $-\mathbf{c}_i \delta t$ , which is an entire number of lattice sites in the direction of  $-\mathbf{c}_i$  (one lattice site for the  $D2Q9$  model, may be one or two sites for a model that consider second neighbors like  $D2Q13$ ).

To write the expression (14) as done in the literature we think of the set of displaced nodes as the original set of nodes  $\mathcal{A}$  plus the set  $\mathcal{G}^i$  of *gained* nodes, this means the set of nodes that would be included in  $\mathcal{A}$  if the body would move by  $-\mathbf{c}_i \delta t$ , minus the set  $\mathcal{L}^i$  of *lost* nodes, this is the set of nodes that would not be included anymore in

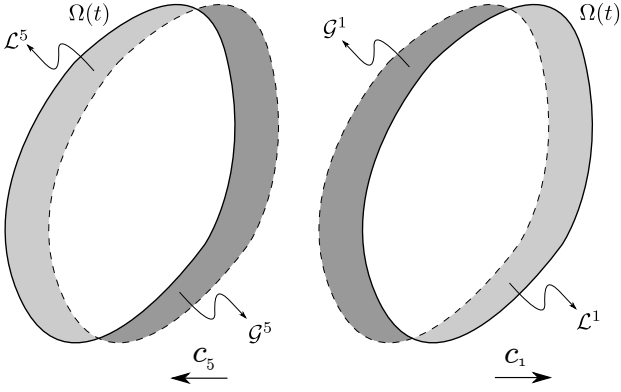


FIG. 2: Schematic domains and areas showing *gained* and *lost* nodes when  $\Omega$  is displaced one lattice site in the  $-\mathbf{c}_5$  (left) and  $-\mathbf{c}_1$  (right) direction in the  $D2Q9$  model. The gray areas are proportional to the size of the sets  $\mathcal{G}^i$  and  $\mathcal{L}^i$ .

$\mathcal{A}$  if the body would move by  $-\mathbf{c}_i\delta t$ . In figure 2 we show an schematic configuration of a fluid system  $\Omega$  and the displaced domains for two particular discrete velocities in a  $D2Q9$  model. Thus, for each discrete velocity direction, we decompose each term of the sum over  $i$  in Eq. (14) as a sum over the set  $\mathcal{A}$  plus what is added from set  $\mathcal{G}^i$  minus what should not be added from set  $\mathcal{L}^i$ . We get

$$\mathbf{F} \simeq \frac{\delta V}{\delta t} \sum_i \mathbf{c}_i \left( \sum_{A \in \mathcal{A}} (\hat{f}_i(\mathbf{x}_A, t) - f_i(\mathbf{x}_A, t)) + \sum_{A \in \mathcal{G}^i} \hat{f}_i(\mathbf{x}_A, t) - \sum_{A \in \mathcal{L}^i} \hat{f}_i(\mathbf{x}_A, t) \right). \quad (15)$$

Notice that, because of (7), the first sum vanishes. Also, all Lattice Boltzmann models are symmetric in the sense that if  $\mathbf{c}_i$  is one of the model's speeds, then  $-\mathbf{c}_i$  is also one of them. Clearly, the lost nodes corresponding to a direction  $i$  are exactly the gained nodes, displaced by an amount  $\mathbf{c}_i\delta t$ , corresponding to the opposite direction and vice versa. Therefore, if we denote with  $\bar{i}$  the index for the opposite direction to  $\mathbf{c}_i$  (i.e.,  $\mathbf{c}_{\bar{i}} = -\mathbf{c}_i$ ), the force can be written as

$$\mathbf{F} \simeq \frac{\delta V}{\delta t} \sum_i \mathbf{c}_i \sum_{A \in \mathcal{G}^i} (\hat{f}_i(\mathbf{x}_A, t) + \hat{f}_{\bar{i}}(\mathbf{x}_A + \mathbf{c}_i\delta t, t)). \quad (16)$$

Equation (16) is precisely the expression that appears extensively in the literature.

## 2. Moving body

When the body moves,  $\Omega(t)$  depends on time and so does set of nodes  $\mathcal{A}_t$ . In this case we denote by  $\mathcal{G}_t^i$  and  $\mathcal{L}_t^i$  the sets of gained and lost nodes by  $\mathcal{A}_t$  if the body would be displaced from its position at time  $t$  by an amount

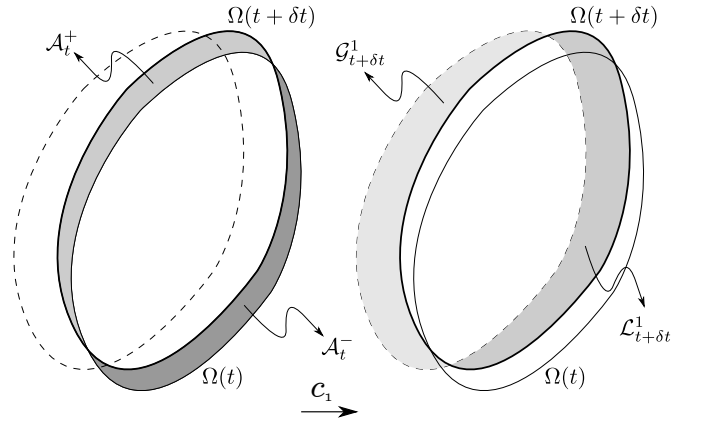


FIG. 3: Schematic domain and areas showing gained and lost nodes for a moving body. Left: gained  $\mathcal{A}_t^+$  and lost  $\mathcal{A}_t^-$  nodes at time  $t + \delta t$ . Right: gained  $\mathcal{G}_{t+\delta t}^i$  and lost  $\mathcal{L}_{t+\delta t}^i$  nodes when  $\Omega(t + \delta t)$  is virtually displaced one lattice site in the  $-\mathbf{c}_1$  direction in the  $D2Q9$  model.

In all cases, the gray areas are proportional to the corresponding sets of nodes.

$-\mathbf{c}_i\delta t$  (see Figure 3, right). Proceeding as done in section III A 1, and considering the time dependence of the sets, equation (13) becomes

$$\mathbf{F} \simeq \frac{\delta V}{\delta t} \sum_i \mathbf{c}_i \left( \sum_{A \in \mathcal{A}_{t+\delta t}} \hat{f}_i(\mathbf{x}_A, t) - \sum_{A \in \mathcal{A}_t} f_i(\mathbf{x}_A, t) + \sum_{A \in \mathcal{G}_{t+\delta t}^i} \hat{f}_i(\mathbf{x}_A, t) - \sum_{A \in \mathcal{L}_{t+\delta t}^i} \hat{f}_i(\mathbf{x}_A, t) \right). \quad (17)$$

For a moving body there is also the real, physical displacement of the body. From  $t$  to  $\delta t$  the real displacement will be smaller than the virtual displacement  $\mathbf{c}_i\delta t$  for any  $i \neq 0$ , because we are assuming a low Mach number flow (see Figure 3, left). For some time steps, one can even expect the set of nodes  $\mathcal{A}_{t+\delta t}$  to be the same as the set of nodes  $\mathcal{A}_t$ . In any case it is useful to define the sets of nodes  $\mathcal{A}_t^+$  and  $\mathcal{A}_t^-$  as

$$\begin{aligned} A \in \mathcal{A}_t^+, & \text{ if } A \in \mathcal{A}_{t+\delta t} \text{ and } A \notin \mathcal{A}_t, \\ A \in \mathcal{A}_t^-, & \text{ if } A \in \mathcal{A}_t \text{ and } A \notin \mathcal{A}_{t+\delta t}. \end{aligned}$$

Then, the first term in Eq. (17) can be expressed as

$$\sum_i \mathbf{c}_i \sum_{A \in \mathcal{A}_{t+\delta t}} \hat{f}_i(\mathbf{x}_A, t) = \sum_i \mathbf{c}_i \left( \sum_{A \in \mathcal{A}_t} \hat{f}_i(\mathbf{x}_A, t) + \sum_{A \in \mathcal{A}_t^+} \hat{f}_i(\mathbf{x}_A, t) - \sum_{A \in \mathcal{A}_t^-} \hat{f}_i(\mathbf{x}_A, t) \right). \quad (18)$$

From (17) and (18) we get

$$\mathbf{F} \simeq \frac{\delta V}{\delta t} \sum_i \mathbf{c}_i \left( \sum_{A \in \mathcal{A}_t^+} \hat{f}_i(\mathbf{x}_A, t) - \sum_{A \in \mathcal{A}_t^-} \hat{f}_i(\mathbf{x}_A, t) + \sum_{A \in \mathcal{G}_{t+\delta t}^i} (\hat{f}_i(\mathbf{x}_A, t) + \hat{f}_{\bar{i}}(\mathbf{x}_A + \mathbf{c}_i \delta t, t)) \right), \quad (19)$$

where we have cancelled out terms by using (7), and have also used that  $\mathbf{c}_{\bar{i}} = -\mathbf{c}_i$ .

Equation (19) is a general expression of the flow force acting over a closed rigid body with general movement. We can identify two different contributions to this force. The last sum is very similar to that of OME, being the difference that the set of nodes is evaluated at  $t + \delta t$ . The first two sums are a contribution to the force that originates in the fact that some lattice nodes enter or leave the body region as it moves around.

A slightly different approximation to the flow force acting on a moving body was presented in [22]. In that work an expression that takes into account the gained and lost nodes is given without theoretical derivation. Nevertheless, the authors find that their proposal is in good agreement with the force computed using other methods.

### B. Fluid torque on the submerged body

To determine the movement of the submerged body we need, besides the total flow force acting on the body, the total flow torque acting on it. In this section we derive an expression for the torque on the rigid body occupying the region  $\Omega(t)$  produced by the fluid flow surrounding this region. We follow the same idea we have used to derive the fluid force and consider the region  $\Omega(t)$  filled with fluid. As before, we assume that the flow is not affected by gravity of other body forces.

The total angular momentum of the fluid system inside  $\Omega(t)$ ,

$$\mathbf{H}(t) = \int_{\Omega(t)} \mathbf{r}(\mathbf{x}) \times \mathbf{u}(\mathbf{x}, t) \rho(\mathbf{x}, t) d\mathbf{x}, \quad (20)$$

where  $\mathbf{r}(\mathbf{x}) = \mathbf{x} - \mathbf{x}_0$  is the position vector with respect to a reference point  $\mathbf{x}_0$ . The flow torque  $\mathbf{T}$  on the fluid system inside  $\Omega(t)$ , with respect to  $\mathbf{x}_0$ , is the time derivative of  $\mathbf{H}$ . Thus

$$\frac{d\mathbf{H}}{dt} = \frac{1}{\delta t} \left( \int_{\Omega(t+\delta t)} \mathbf{r}(\mathbf{x}) \times (\mathbf{u}\rho)(\mathbf{x}, t + \delta t) d\mathbf{x} - \int_{\Omega(t)} \mathbf{r}(\mathbf{x}) \times (\mathbf{u}\rho)(\mathbf{x}, t) d\mathbf{x} \right) + \mathcal{O}(\delta t). \quad (21)$$

Proceeding as in section III A, we use Eq. (3) and approximate space integrals by sums over the lattice. We

have from Eq. (21)

$$\mathbf{T} \simeq \frac{\delta V}{\delta t} \sum_i \left( \sum_{A \in \mathcal{A}_{t+\delta t}} \mathbf{r}(\mathbf{x}_A) \times \mathbf{c}_i \hat{f}_i(\mathbf{x}_A - \mathbf{c}_i \delta t, t) - \sum_{A \in \mathcal{A}_t} \mathbf{r}(\mathbf{x}_A) \times \mathbf{c}_i f_i(\mathbf{x}_A, t) \right). \quad (22)$$

Equation (22) gives the total fluid flow torque on the fluid system  $\Omega(t)$  with respect to a reference point  $\mathbf{x}_0$ . As we have done for the force evaluation, we give explicitly the expression to evaluate the torque acting on static and moving bodies.

#### 1. Static body

If the body doesn't move, the geometric variables are time independent. Then, from the Eq. (22) we have

$$\mathbf{T} \simeq \frac{\delta V}{\delta t} \sum_i \sum_{A \in \mathcal{A}} \mathbf{r}(\mathbf{x}_A) \times \mathbf{c}_i \left( \hat{f}_i(\mathbf{x}_A - \mathbf{c}_i \delta t, t) - f_i(\mathbf{x}_A, t) \right). \quad (23)$$

We rewrite the term with  $\hat{f}_i$  as done in section III A 1, and use the same definition for the sets  $\mathcal{G}^i$  and  $\mathcal{L}^i$ , (see Figure 2). We have

$$\begin{aligned} & \sum_i \sum_{A \in \mathcal{A}} \mathbf{r}(\mathbf{x}_A) \times \mathbf{c}_i \hat{f}_i(\mathbf{x}_A - \mathbf{c}_i \delta t, t) = \\ & \sum_i \left( \sum_{A \in \mathcal{A}} \mathbf{r}(\mathbf{x}_A) \times \mathbf{c}_i \hat{f}_i(\mathbf{x}_A, t) + \sum_{A \in \mathcal{G}^i} \mathbf{r}(\mathbf{x}_A) \times \mathbf{c}_i \hat{f}_i(\mathbf{x}_A, t) - \sum_{A \in \mathcal{L}^i} \mathbf{r}(\mathbf{x}_A) \times \mathbf{c}_i \hat{f}_i(\mathbf{x}_A, t) \right). \end{aligned}$$

Thus, from equation (23), we get

$$\begin{aligned} \mathbf{T} \simeq \frac{\delta V}{\delta t} \sum_i \left( \sum_{A \in \mathcal{A}} \mathbf{r}(\mathbf{x}_A) \times \mathbf{c}_i \left( \hat{f}_i(\mathbf{x}_A, t) - f_i(\mathbf{x}_A, t) \right) + \sum_{A \in \mathcal{G}^i} \mathbf{r}(\mathbf{x}_A) \times \mathbf{c}_i \hat{f}_i(\mathbf{x}_A, t) - \sum_{A \in \mathcal{L}^i} \mathbf{r}(\mathbf{x}_A) \times \mathbf{c}_i \hat{f}_i(\mathbf{x}_A, t) \right). \quad (24) \end{aligned}$$

Notice that, from Eq. (7), the first sum vanishes. As before, we denote by  $\bar{i}$  the direction opposite to  $i$ , then

$$\mathbf{T} \simeq \frac{\delta V}{\delta t} \sum_i \sum_{A \in \mathcal{G}^i} \mathbf{r}(\mathbf{x}_A) \times \mathbf{c}_i \left( \hat{f}_i(\mathbf{x}_A, t) + \hat{f}_{\bar{i}}(\mathbf{x}_A + \mathbf{c}_i \delta t, t) \right). \quad (25)$$

As for the force, we have a sum over the nodes  $A \in \mathcal{G}^i \forall i$ , which are the first neighbor nodes to surface  $\partial\Omega$ . Equation (25) is presented in the literature as the expression

to evaluate the torque on a submerged body using OME. Our derivation makes clear that this expression is valid for static bodies. For moving bodies we obtain corrections to (25).

## 2. Moving body

For a moving body, as we have seen in section III A 2, the sets  $\Omega(t)$ ,  $\mathcal{A}_t$  and the sets of gained and lost nodes  $\mathcal{G}_t^i$  and  $\mathcal{L}_t^i$  depend on time. Recalling the definitions of  $\mathcal{A}_t^+$  and  $\mathcal{A}_t^-$ , we get from (22)

$$\begin{aligned} \mathbf{T} \simeq & \frac{\delta V}{\delta t} \sum_i \left( \sum_{A \in \mathcal{A}_t^+} \mathbf{r}(\mathbf{x}_A) \times \mathbf{c}_i \hat{f}_i(\mathbf{x}_A, t) \right. \\ & - \sum_{A \in \mathcal{A}_t^-} \mathbf{r}(\mathbf{x}_A) \times \mathbf{c}_i \hat{f}_i(\mathbf{x}_A, t) + \sum_{A \in \mathcal{G}_{t+\delta t}^i} \mathbf{r}(\mathbf{x}_A) \times \mathbf{c}_i \hat{f}_i(\mathbf{x}_A, t) \\ & \left. - \sum_{A \in \mathcal{L}_{t+\delta t}^i} \mathbf{r}(\mathbf{x}_A) \times \mathbf{c}_i \hat{f}_i(\mathbf{x}_A, t) \right). \end{aligned} \quad (26)$$

where Eq. (7) was used to eliminate the sum over the set  $\mathcal{A}$ . We obtain

$$\begin{aligned} \mathbf{T} \simeq & \frac{\delta V}{\delta t} \sum_i \left( \sum_{A \in \mathcal{A}_t^+} \mathbf{r}(\mathbf{x}_A) \times \mathbf{c}_i \hat{f}_i(\mathbf{x}_A, t) \right. \\ & - \sum_{A \in \mathcal{A}_t^-} \mathbf{r}(\mathbf{x}_A) \times \mathbf{c}_i \hat{f}_i(\mathbf{x}_A, t) \\ & \left. + \sum_{A \in \mathcal{G}_{t+\delta t}^i} \mathbf{r}(\mathbf{x}_A) \times \mathbf{c}_i \left( \hat{f}_i(\mathbf{x}_A, t) + \hat{f}_i(\mathbf{x}_A + \mathbf{c}_i \delta t, t) \right) \right). \end{aligned} \quad (27)$$

Thus, the torque acting on a moving fluid system is the sum of two different contributions. On the one hand, a contribution coming from the nodes that arrive ( $\mathcal{A}_t^+$ ) and leave ( $\mathcal{A}_t^-$ ) the system region  $\Omega(t + \delta t)$ . On the other hand, a contribution of momentum exchange applied to the fluid system at time  $t + \delta t$ .

Equation (27) is different than the OME expression to evaluate the torque. We find in our simulations that our expression gives more accurate results than OME (see Section IV).

## IV. NUMERICAL TESTS

In this section we check the expressions derived in section III to compute the force and torque acting on a submerged body, hereafter *corrected momentum exchange (CME)*. To this end we perform three benchmark tests on well known problems that have been tested and benchmarked widely with others computational fluid dynamics (CFD) methods, such as finite element method (FEM) and finite difference methods.

We are interested in analyzing the dynamics of single bodies and a pair of rigid bodies sedimenting across a vertical channel filled with a Newtonian fluid. The bodies are either circular or elliptic discs. The accuracy in the determination of the force and torque acting on the falling body directly affects the body's movement. If the force and torque are computed correctly, the displacement and rotation of the discs across the domain should be in agreement with data presented in the literature [4, 15, 21, 22, 24].

To solve the flow we use a  $D2Q9$  lattice scheme and SRT with  $\tau = 0.6$ . The fluid density and the kinematic viscosity are set to  $\rho_f = 1000 \text{ kg/m}^3$  and  $\nu = 1 \times 10^{-6} \text{ m}^2/\text{s}$  respectively. The fluid is initially at rest and has zero velocity at the horizontal and vertical boundaries at all times. We implement these boundary conditions with the method presented in [25]. The acceleration of gravity acting on the body is  $g = 9.81 \text{ m/s}^2$  downwards.

The motion of each body is determined by integrating Newton's equation of motion, where the force is given by the fluid flow force, weight and buoyancy force. To integrate in time we use Euler Forward numerical scheme, which is first order accurate as the LBM method and CME method itself.

### A. Sedimentation of a circular disc

In this benchmark test we analyze the dynamics of a single two-dimensional disc sedimenting across a vertical channel, shown schematically in figure 4. We test the dynamics of the disc for two density relations  $r_\rho = \rho_b/\rho_f$ , with  $\rho_b$  and  $\rho_f$  the densities of the body (disc) and the fluid respectively.

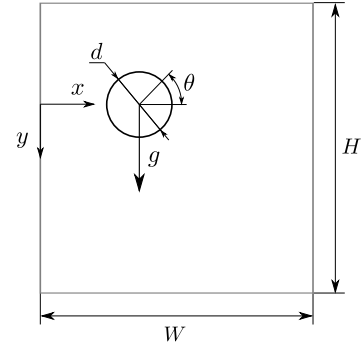


FIG. 4: An schematic diagram of the sedimentation discs problem configuration

The dimensions of the vertical channel are  $W = 4d$  and  $H = 8W$ ; the disc diameter is  $d = 1 \times 10^{-3} \text{ m}$ . The disc center is initially placed at  $(x, y) = (7.6 \times 10^{-4}, 0) \text{ m}$  with the coordinate origin at  $2.5 \times 10^{-2} \text{ m}$  from the bottom of the channel and placed as shows the figure 4. We discretized the computational domain with  $n_x \times n_y = 135 \times 1073$  lattice points.

We test the performance of the method for two density ratios  $r_\rho = 1.01$ , and  $1.03$ . In Figures 5 and 6 we show the horizontal and vertical velocities and the trajectory

of the center of the disc and the rotation angle of the disc as functions of time, for  $r_\rho = 1.01$  and  $r_\rho = 1.03$ .

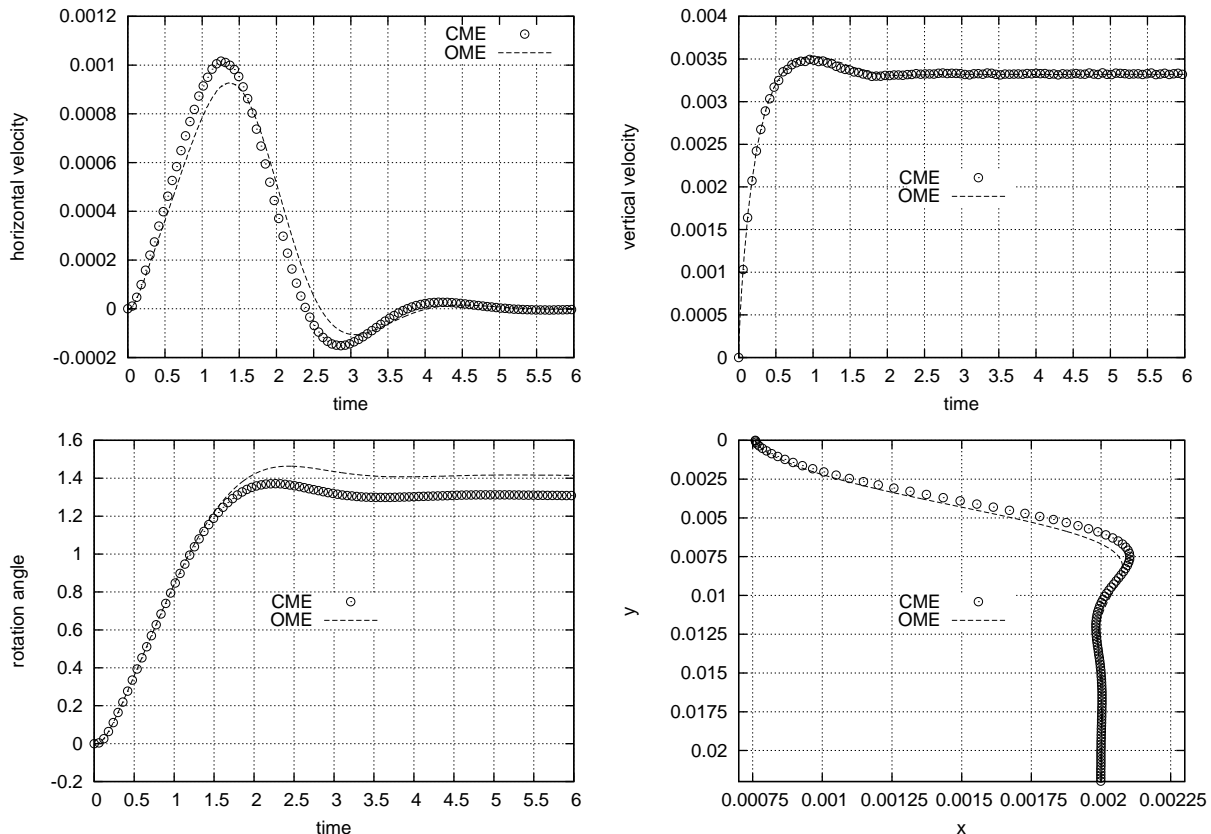


FIG. 5: Results obtained for the sedimenting disc of Figure 4 for  $r_\rho = 1.01$ . All magnitudes are expressed in the international system of units.

When the disc is released from the initial position at  $t = 0$ , it starts moving and rotating across the channel. As one can see in the figures, the movement of the disc can be divided into two regimes: A transient and a stationary regime.

We compare the results we obtained using both OME and CME. Our results, particularly the one obtained with CME, are in good agreement with tests presented in [15] (obtained using LBM with SI), [22] (obtained using LBM with corrected ME) and [4] (obtained using FEM). We observe visible discrepancies between CME and OME, particularly for the horizontal velocity and position. The major discrepancy shows in the transient regime; no significant discrepancies can be seen in the stationary regime. Similar observations have been made by Wen et. al. [22] and Li et. al [15].

## B. Sedimentation of an elliptic disc

In this section we present a benchmark test, similar to the previous one, where the circular disc is replaced with an elliptical disc, also sedimenting in a vertical channel filled with Newtonian fluid. This test is also widely analyzed in the literature. We study a problem as the one presented by Xia et. al. [24], where the authors use LBM and SI to obtain the forces on the body.

We show in Figure 7 a schematic diagram of the problem. We define three dimensionless parameters that characterize the problem. These parameters are the aspect ratio  $\alpha = a/b$ , with  $a$  and  $b$  the major and minor axes of the ellipse respectively, the blockage ratio  $\beta = W/a$ , with  $W$  the width of the vertical channel, and the density ratio  $r_\rho$  as defined in Section IV A.

An exhaustive analysis of this sedimentation problem



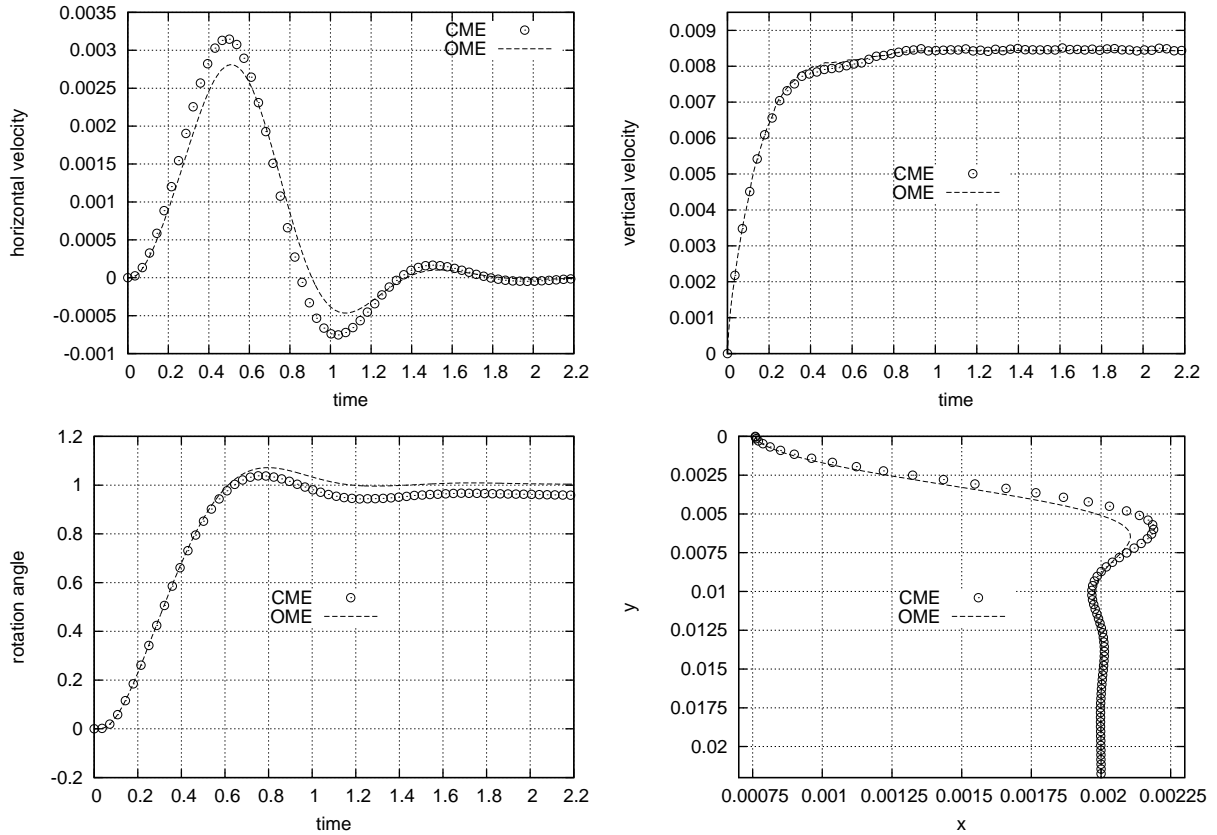


FIG. 6: Results obtained for the sedimenting disc of Figure 4 for  $r_\rho = 1.03$ . All magnitudes are expressed in the international system of units.

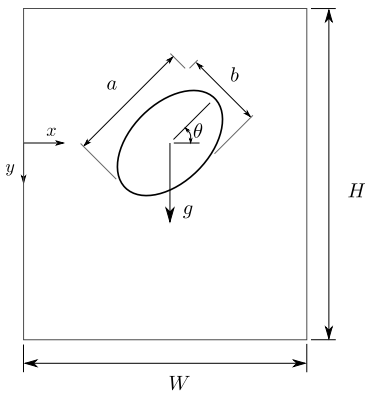


FIG. 7: An schematic diagram of the single two-dimensional elliptical particle sedimenting in a vertical channel.

was carried out by Xia et. al. [24]. They studied the influence on the dynamics of the density ratio, the aspect ratio, and the channel blockage ratio. For simplicity we analyze this problem with a fix blockage ratio, chosen so that we don't need to consider the wall-particle interaction. Our interest is to test the method proposed in the

present work, not to give a complete description of the sedimentation problem. We carry out simulations with a fixed geometrical configuration and for four density ratios.

In our tests we use major axis  $a = 1 \times 10^3 \text{m}$ , aspect ratio  $\alpha = 2$  and blockage ratio  $\beta = 4.0$ . The properties of the fluid are the same used in Section IV A. Initially, the fluid is at rest, the center of the ellipse is placed at  $(x, y) = (0.5W, 0) \text{m}$ . The coordinate origin at  $4.8 \times 10^{-2} \text{m}$  from the bottom of the vertical channel. To break the symmetry of the problem, we choose an initial angular position  $\theta_0 = \frac{\pi}{4}$ . We set, following [24], a height  $H = 50a$  and a width  $W = 4a$ . The domain is discretized in a lattice with  $n_x \times n_y = 135 \times 1676$  points. We make runs for four density ratios  $r_\rho = 1.01, 1.10, 1.30$  and  $1.50$ .

In the Figure 8 we show the result of our simulation using CME for  $r_\rho = 1.10$ . This result is compared with the one we obtained using OME. In Figure 9 we show our results for density relations  $r_\rho = 1.01, 1.10, 1.30$  and  $1.50$ , where the dynamical variables are given as a function of time and the complete trajectory of the ellipse is also shown. Our results using CME are in good agreement with the results of Xia et. al. [24]. It is clear from Figure 8, that there exists an important difference, in the transient regime, with the results obtained using OME.

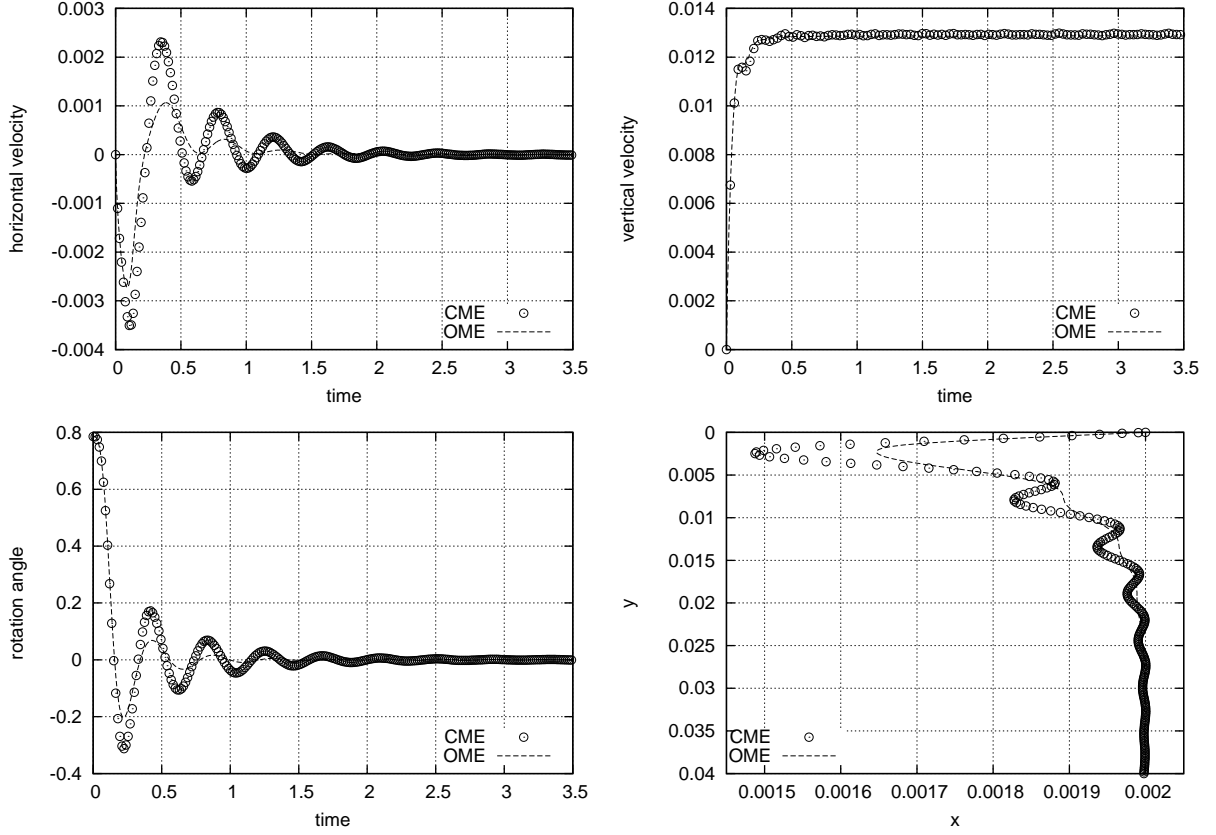


FIG. 8: Results for the sedimenting elliptic disk test of Figure 7. Comparison between CME and OME methods for the case  $r_\rho = 1.10$ . All magnitudes are expressed in the international system of units.

### C. Sedimentation of two circular discs—Pure wake interaction

In this section we present a benchmark test where two circular discs with different densities sediment in a vertical channel. We label the discs as 1 and 2, and place them in the vertical channel, at  $t = 0$ , as shown in Figure 10. The setting of the problem is such that no direct contact between the discs or with the walls occur as a consequence of time evolution.

This problem has been tested by Uhlmann [21] using a finite difference scheme to solve the Navier-Stokes equation. We choose this as a simple problem where a complex interaction between the discs occurs. This interaction is mediated by the flow field only so that a collision model is not needed.

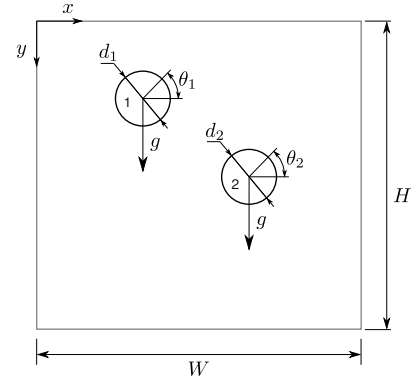


FIG. 10: An schematic diagram of the two-discs particle sedimenting in a vertical channel in pure wake interaction.

The dimensions of the vertical channel are  $W = 2$  m and  $H = 10$  m. The diameter of the discs are  $d_1 = d_2 = 0.2$  m, where the subindex makes reference to the disc label. The density ratio are  $r_{\rho_1} = 1.5$ , and

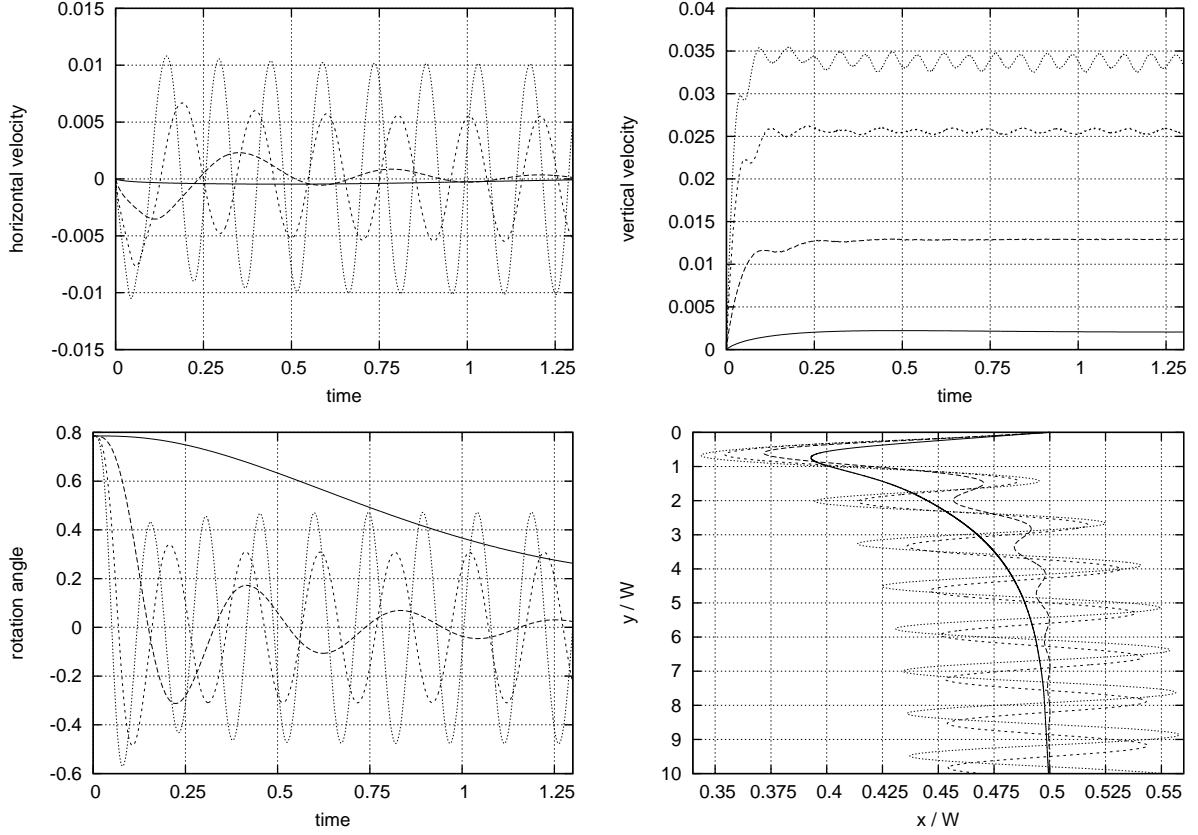


FIG. 9: Results for the sedimenting elliptic disk test of Figure 7, using CME, for four different density ratios. In all plots the continuous line is used for  $r_\rho = 1.01$ , the long-dashed line for  $r_\rho = 1.10$ , the short-dashed line for  $r_\rho = 1.30$  and the dotted line for  $r_\rho = 1.50$ .

$r_{\rho_2} = 1.25$ . The centers of the discs are initially placed at  $(x, y)_1 = (0.87, 0.8)$  m and  $(x, y)_2 = (1.13, 1.2)$  m, as shown in Figure 10, being the coordinate origin placed at the upper left corner of the domain. The fluid viscosity is set as  $\nu = 8 \times 10^{-4}$  m<sup>2</sup>/s. We set a lattice with  $n_x \times n_y = 485 \times 4171$ , that give us a relation  $d/\delta x \approx 48$ , similar to that used in [21]. Both discs and fluid are completely at rest at  $t < 0$ ; the discs are released at initial time  $t = 0$  and start moving under the action of gravity.

The results of our simulation using CME are shown in figures 11 and 12. Our simulation runs until  $t = 8.5$  when the heavier disc arrive to the bottom of the boundary domain. In Figure 11 the trajectories of the centers of both discs are shown. The influence of the interaction of the discs and flow is clearly notable. The distortion of the trajectory is much larger on the lighter disc. In the heavier disc trajectory, the “oscillations” are larger at the beginning, when the disc is higher in altitude and then more influenced by the lighter disc wake. In Figure 12 we show the vertical and horizontal displacements and velocities of both discs as function of time. Our results show a qualitative agreement with those presented in [21]. We can observe however some minor discrepan-

cies, particularly on the horizontal velocity of the lighter disc.

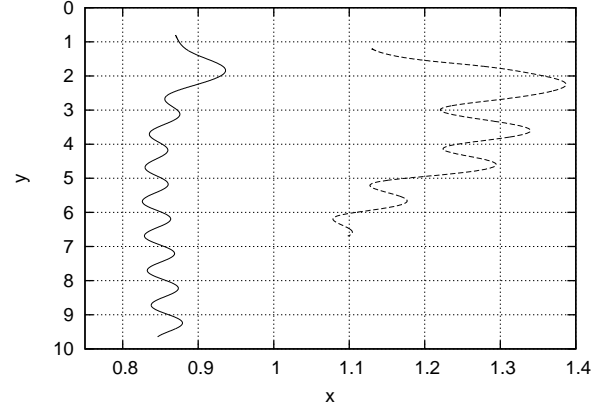


FIG. 11: Trajectory of the sedimenting disc centers of Figure 10. Continuous line for disc 1 and dashed line for disc 2.

## V. CONCLUSION AND DISCUSSION

In this work we have presented a new derivation of the momentum exchange method to compute the flow force

and torque acting on a submerged body. The expressions

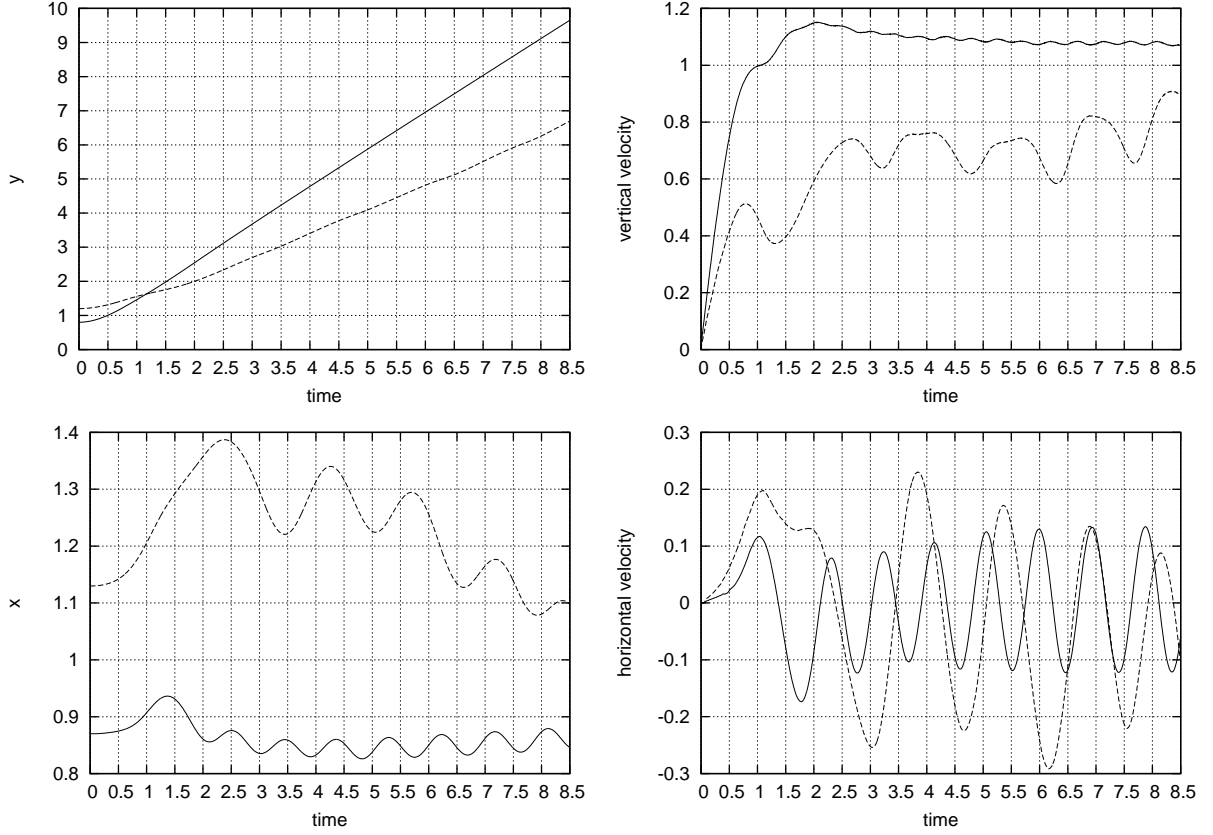


FIG. 12: Results for the sedimenting discs test of Figure 10. Vertical positions (upper left plot), vertical velocities (upper right plot), horizontal positions (lower left plot) and horizontal speed (lower right plot).

we obtain are coincident with the original Ladd's algorithm for the case of static bodies. Our derivation gives, in turn, corrected formulas for the case of moving bodies. Even when in this work we concentrate on rigid bodies, the formulas we find for the case of moving bodies are also valid for non-rigid bodies.

Our method of deriving momentum exchange does not use a particular treatment of the boundary conditions on the body surface. The expressions obtained for the flow force and torque can be applied with several of the various methods proposed in the literature to treat the boundary conditions, as long as the boundary conditions are correct in the sense that no mass transfer occur across the boundary of the body.

In the last part of the paper we have tested the corrected momentum exchange expressions we obtained by simulating three problems which are well known in the literature, a sedimenting circular disc, a sedimenting elliptic disc and two sedimenting circular discs. Our results clearly show the difference between the results of the corrected momentum exchange as compared to those of the

original algorithm for the case of moving bodies. The results of our corrected expressions are in good agreement with those obtained by other authors using similar and different computational fluid dynamic methods such as finite element methods.

An interesting step to follow would be to simulate a non-trivial dynamical problem where experimental data are available. We are working on one such problem on a three dimensional setting and where we implement mesh (or lattice) refinement. The results we obtain will be reported in a future work.

### Acknowledgments

We want to thank Carlos Sacco and Ezequiel Malamud for useful discussions. J. P. Giovacchini is a fellowship holder of CONICET (Argentina). This work was supported in part by grants 05-B454 of SECyT, UNC and PIDDEF 35-12 (Ministry of Defense, Argentina).

---

[1] P. L. Bhatnagar, E. P. Gross, and M. Krook. A model for collision processes in gases. i. small amplitude processes

in charged and neutral one-component systems. *Phys.*

- Rev.*, 94:511–525, May 1954.
- [2] A. Caiazzo. Analysis of lattice boltzmann nodes initialization in moving boundary problems. 2007.
  - [3] A. Caiazzo and M. Junk. Boundary force in lattice boltzmann: Analysis of momentum exchange algorithm. *Computers and Mathematics with Applications*, 55:1415–1423, 2008.
  - [4] J. Feng, H. H. Hu, and D. D. Joseph. Direct simulation of initial value problems for the motion of solid bodies in a newtonian fluid part 1. sedimentation. *Journal of Fluid Mechanics*, 261:95–134, 1994.
  - [5] O. Filippova and D. Hänel. Grid refinement for lattice-bgk models. *Journal of Computational Physics*, 147(219), 1998.
  - [6] R. W. Fox, A. T. McDonald, and P. J. Pritchard. *Introduction to Fluid Mechanics*. John Wiley & Sons, 6 edition, 2004.
  - [7] S. Harris. *An Introduction to the Theory of the Boltzmann Equation*. Dover books on physics. Dover Publications, 2004.
  - [8] X. He and L.-S. Luo. Lattice boltzmann model for the incompressible navierstokes equation. *Journal of Statistical Physics*, 88(3-4):927–944, 1997.
  - [9] X. He and L.-S. Luo. Theory of the lattice boltzmann method: From the boltzmann equation to the lattice boltzmann equation. *Phys. Rev. E*, 56(6):6811–6817, Dec 1997.
  - [10] X. He and L.-S. Luo. Theory of the lattice boltzmann method: From the boltzmann equation to the lattice boltzmann equation. *Phys. Rev. E*, 56(6):6811–6817, 1997.
  - [11] T. Inamuro, K. Maeba, and F. Ogino. Flow between parallel walls containing the lines of neutrally buoyant circular cylinders. *International Journal of Multiphase Flow*, 26(12):1981 – 2004, 2000.
  - [12] A. J. C. Ladd. Numerical simulations of particulate suspensions via a discretized boltzmann equation. part 1. theoretical foundation. *Journal of Fluid Mechanics*, 271:285–309, 7 1994.
  - [13] A. J. C. Ladd. Numerical simulations of particulate suspensions via a discretized boltzmann equation. part 2. numerical results. *Journal of Fluid Mechanics*, 271:311–339, 7 1994.
  - [14] P. Lallemand and L.-S. Luo. Lattice boltzmann method for moving boundaries. *Journal of Computational Physics*, 184(2):406 – 421, 2003.
  - [15] H. Li, X. Lu, H. Fang, and Y. Qian. Force evaluations in lattice boltzmann simulations with moving boundaries in two dimensions. *Phys. Rev. E*, 70:026701, Aug 2004.
  - [16] R. Mei, L.-S. Luo, and W. Shyy. An accurate curved boundary treatment in the lattice boltzmann method. *Journal of Computational Physics*, 155(2):307 – 330, 1999.
  - [17] R. Mei, W. Shyy, D. Yu, and L.-S. Luo. Lattice boltzmann method for 3-d flows with curved boundary. *Journal of Computational Physics*, 161(2):680 – 699, 2000.
  - [18] R. Mei, D. Yu, W. Shyy, and L.-S. Luo. Force evaluation in the lattice boltzmann method involving curved geometry. *Phys. Rev. E*, 65(041203), 2002.
  - [19] Y. Sone. *Molecular Gas Dynamics: Theory, Techniques, and Applications*. Modeling and Simulation in Science, Engineering and Technology. Springer London, Limited, 2007.
  - [20] S. Succi. *The lattice Boltzmann equation for fluid dynamics and beyond*. Numerical Mathematics and Scientific Computation. Oxford University Press, Oxford, 2001.
  - [21] M. Uhlmann. An immersed boundary method with direct forcing for the simulation of particulate flows. *J. Comput. Phys.*, 209(2):448–476, Nov. 2005.
  - [22] B. Wen, H. Li, C. Zhang, and H. Fang. Lattice-type-dependent momentum-exchange method for moving boundaries. *Phys. Rev. E*, 85:016704, Jan 2012.
  - [23] D. Wolf-Gladrow. *Lattice-Gas Cellular Automata and Lattice Boltzmann Models: An Introduction*. Number n.º 1725 in Lattice-gas Cellular Automata and Lattice Boltzmann Models: An Introduction. Springer, 2000.
  - [24] Z. Xia, K. W. Connington, S. Rapaka, P. Yue, J. J. Feng, and S. Chen. Flow patterns in the sedimentation of an elliptical particle. *Journal of Fluid Mechanics*, 625:249–272, 4 2009.
  - [25] Q. Zou and X. He. On pressure and velocity boundary conditions for the lattice boltzmann bgk model. *Phys. Fluids E*, 9(6):1591–1598, 1997.
  - [26] In incompressible-flow models, the same relation between  $\delta x$  and  $\delta t$  holds, but the constant  $c$  is no longer related to the speed of sound.
  - [27] The first method proposed to impose boundary conditions in LBM is known as bounce-back. Bounce-back was appropriate to treat rectilinear boundaries which are aligned with the lattice. The application of bounce-back when the boundary is of general shape would be equivalent to approximate the boundary of the body by a stair-step shape boundary coincident with lattice links, which implies a loose of accuracy.
  - [28] If one thinks of the nodes at the center of elementary volume cells, the integrals are approximated by the mid-point rule, which is second order accurate when  $\Omega$  is an exact number of cells. The accuracy is lower on more general domains.